Astron. Astrophys. 356, L45–L48 (2000)

ASTRONOMY AND ASTROPHYSICS

LETTER

Letter to the Editor

The first radius-expansion X-ray burst from GX 3+1

E. Kuulkers[1,2] **and M. van der Klis**[3]

[1] Space Research Organization Netherlands, Sorbonnelaan 2, 3584 CA Utrecht, The Netherlands (E.Kuulkers@sron.nl)
[2] Astronomical Institute, Utrecht University, P.O. Box 80000, 3507 TA Utrecht, The Netherlands
[3] University of Amsterdam, Astronomical Institute "Anton Pannekoek", and Center for High Energy Astrophysics, Kruislaan 403, 1098 SJ Amsterdam, The Netherlands (michiel@astro.uva.nl)

Received 21 February 2000 / Accepted 13 March 2000

Abstract. During several observations in 1999 August with RXTE of the low-mass X-ray binary GX 3+1, we found a single short and strong X-ray burst. This is the first burst from GX 3+1 which clearly shows evidence for radius expansion of the neutron-star photosphere during the thermo-nuclear runaway. We show that the cooling phase of the neutron star photosphere starts already just before the end of the contraction phase. Considering the fact that the radius expansion is due to the burst luminosity being at the Eddington luminosity, assuming standard burst parameters and accounting for gravitational redshift effects we derive a distance to the source of $\sim$4.5 kpc, although relaxing these assumptions may lead to uncertainties up to $\sim$30%. By comparing the persistent flux with that observed at the peak of the burst we infer that near the time of the X-ray burst the persistent luminosity of GX 3+1 is $\sim 0.17\,L_{\rm edd}$, confirming predictions from theoretical modeling of X-ray spectra of bright sources like GX 3+1.

Key words: accretion, accretion disks – stars: binaries: close – stars: individual: – stars: neutron – X-rays: bursts

1. Introduction

The overall X-ray intensity of the low-mass X-ray binary (LMXB) GX 3+1 varies slowly on time scales of months to years (Makishima et al. 1983; Asai et al. 1993, see also Fig. 1). X-ray bursts in GX 3+1 were discovered by *Hakucho*, at a time when the persistent X-ray flux was about half of that seen previously (Makishima et al. 1983). During that time roughly one burst per day was observed. The bursts from this source were shown to be thermonuclear flashes on the neutron star surface, i.e. being of type I (Makishima et al. 1983; Asai et al. 1993: *Ginga*; Molkov et al. 1999: *GRANAT/ART-P*), but none of them showed evidence for photospheric radius expansion.

GX 3+1 is one of the four brightest so-called "atoll" sources (Hasinger & van der Klis 1989). The sources in this group (including GX 13+1, GX 9+1 and GX 9+9) hardly show any X-ray bursts (if at all), and display properties like those of other atoll sources when these are in their high accretion rate state: their tracks in X-ray colour-colour diagrams are long, diagonal and slightly curved, while their fast timing properties are at all times dominated by a relatively weak (1–4% rms) power-law shaped noise component. Detailed X-ray spectral modeling seems to suggest that they accrete with rates near 10% of the Eddington mass accretion rate, i.e. intermediate between the more frequently bursting atoll sources and that of the so-called "Z" sources (Psaltis & Lamb 1998). At low accretion rates (and therefore probably low intensities) such sources are predicted to display the properties characteristic of the more frequently bursting atoll sources, which in view of the Hakucho result (see above) at least GX 3+1 seems to satisfy.

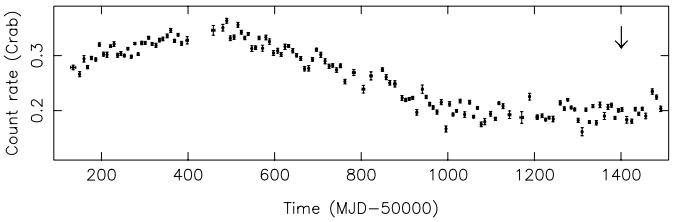

Fig. 1. ASM light curve (2–12 keV) of GX 3+1 from 1996 January 12 to 1999 December 31 in units of the Crab count rate ($\sim$75 cts s^{-1} SSC^{-1}). The data points represent the mean of 8 consecutive daily averages. The time of the burst observed with the PCA is indicated by an arrow.

During one of our series of target of opportunity observations with RXTE aimed at observing GX 3+1 at low intensities, we observed a strong ($\sim$2.3 Crab [2–10 keV] at maximum) and short (15–20 s) X-ray burst. The burst onset occurred on 1999 August 10, 18:35:53.5 UTC. In this paper we discuss its properties.

2. Observations and analysis

Data were acquired with the Proportional Counter Array (PCA; Bradt et al. 1993) in various observation modes. During our observation from 1999 August 10, 17:15 to August 11, 00:00 UTC, only three units were active, i.e. PCU0, PCU2 and PCU3. For

Send offprint requests to: Erik Kuulkers

the spectral analysis of the persistent emission we used data collected in 16 s intervals with 129 spectral channels. We accumulated data stretches of 96 s just before and after the burst, combining the three PCU's. In order to study the burst properties we used a mode which provides 64 spectral channels at a time resolution of 16 μs; this mode combines information from all PCU's. Spectra during the burst were determined every 0.25 sec during the first 10 s, and every 0.5 s for the remainder. All spectra were corrected for background and dead-time using the procedures supplied by the RXTE Guest Observer Facility. A systematic uncertainty of 1% was taken into account. For our spectral fits we confined the energy range to 2.9–20 keV. The hydrogen column density, N_H, towards GX 3+1 was fixed to that found by the *Einstein* SSS and MPC measurements ($1.7{\cdot}10^{22}$ atoms cm^{-2}, Christian & Swank 1997).

Large amplitude, high coherence brightness oscillations have been observed during various X-ray bursts in other LMXBs (see Strohmayer 1998, 2000). In our search for possible burst oscillations we made fast Fourier transforms (FFTs) of data segments ranging from 0.25 s to 2 s long during the burst, with time steps of 0.125 s (so-called sliding FFTs). We used the 64 spectral channel and 16 μsec data set, and limited our search to the 50 to 2048 Hz frequency range. We performed the search in the whole PCA energy range (2–60 keV), as well as in a relatively high energy range (8–60 keV).

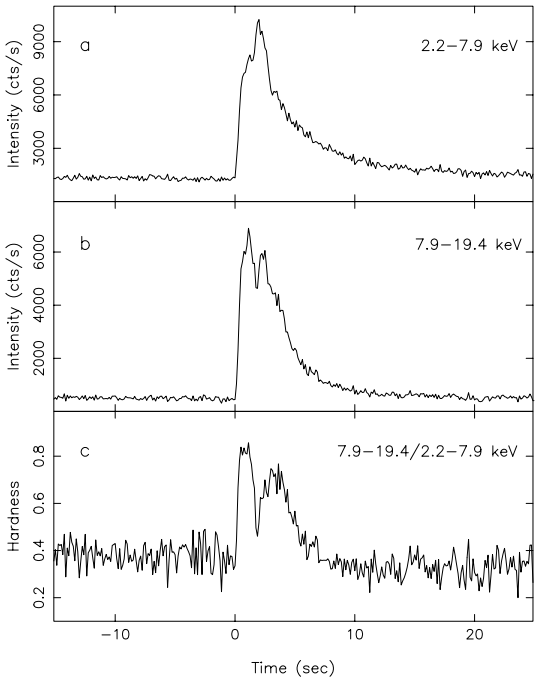

Fig. 2a–c. The X-ray burst light curve at low (**a**) and high (**b**) energies and the corresponding hardness curve (**c**), all at a time resolution of 0.125 sec. T=0 s corresponds to 1999 August 10, 18:35:53.5 UTC.

3. Results

3.1. Temporal behaviour

The light curve of the burst at low energies is single-peaked, whereas at high energies it is double-peaked (Fig. 2a,b). The corresponding hardness curve (Fig. 2c) shows that the burst first hardens, softens, hardens again, and then gradually softens again. Our search for burst oscillations yielded negative results. Previous burst oscillations were found mainly during the rise to burst maximum and after the radius-expansion phase (see Strohmayer 1998, 2000). Using the 0.25 s long FFTs in the full energy range, we derive upper limits on the modulation amplitude of burst oscillations of $\sim$45% at the start of the rise, $\sim$15% at the maximum of the burst, and $\sim$20% just after the radius expansion phase. The upper limits in the 8–60 keV energy band are $\sim$60%, $\sim$20%, and $\sim$25%, respectively. The 2 s long FFTs give more stringent upper limits of $\sim$16%, $\sim$6%, and $\sim$9%, respectively, for the full energy range, whereas we derive $\sim$24%, $\sim$7%, and $\sim$10%, respectively, in the 8–60 keV energy band.

3.2. Spectral behaviour

The net burst spectra (i.e. total burst spectrum minus persistent spectrum) were satisfactorily ($\chi^2_{\rm red}$ less than $\sim$2) modeled by black-body emission. The results are shown in Fig. 3. A dip in the black-body temperature, $T_{\rm bb}$, $\sim$2 s after the burst onset is apparent, simultaneous with an increase of a factor of $\sim$2 in the black-body radius, $R_{\rm bb}$. The total increase/decrease phase of $R_{\rm bb}$ lasts only $\sim$1.5 sec.

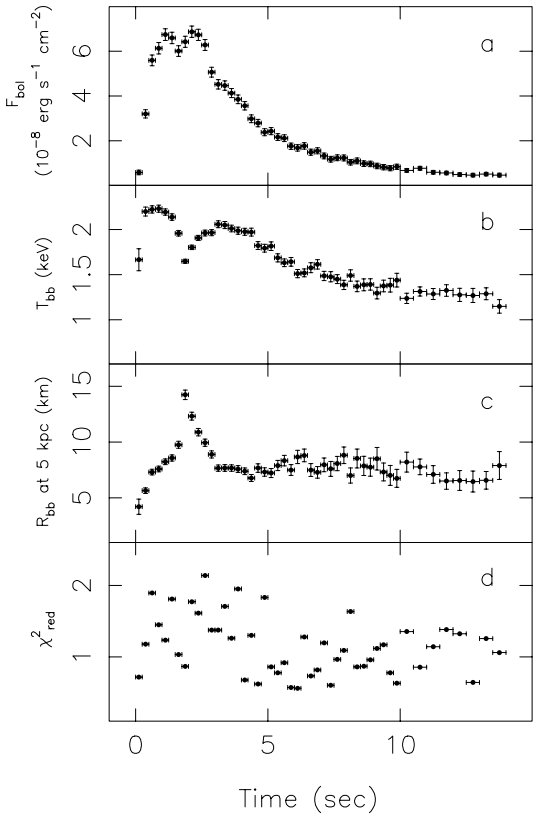

Fig. 3a–d. Spectral fit results during the burst: (**a**) bolometric black-body flux, $F_{\rm bol}$, (**b**) black-body temperature, $T_{\rm bb}$, (**c**) effective black-body radius, $R_{\rm bb}$, at 5 kpc, and (**d**) goodness of fit expressed in reduced χ^2.

We note that the X-ray spectral analysis during bursts can be significantly hampered when the persistent emission contains a black-body contribution from the same surface of the neutron star that emits the burst emission (van Paradijs & Lewin 1985). In that case our spectral fits to the net burst spectra may contain systematic errors in the black-body temperature and radius, especially near the end of the burst. We therefore repeated our spectral analysis to the total burst spectra, fixing the non black-body component in the persistent emission (see Table 1). The black-body component, which now includes all emission from the neutron star surface, is left free. This procedure only slightly alters our estimated black-body flux. The absence of significant differences between the two methods is mainly due the fact that the burst is sufficiently stronger than the persistent emission (which is reflected by the burst parameter γ, see below), as also noted by Asai et al. (1993).

The persistent emission just before and after the burst can be satisfactorily modeled by a black-body plus a cut-off power-law component (Table 1). Using the X-ray spectral fits we can determine the peak flux (i.e. including persistent emission), $F_{\rm peak}$, and the total burst fluence (i.e. the integrated net burst flux), $E_{\rm b}$, and hence the burst parameters γ (=$F_{\rm pers}$/[$F_{\rm peak}$-$F_{\rm pers}$]) and τ (=$E_{\rm b}$/$F_{\rm peak}$). For the burst parameter α (=$F_{\rm pers}$/($E_{\rm b}$/Δt)), where Δt is the time since the previous burst) we can only give a lower limit, since the source is not observed during South Atlantic Anomaly passages and earth occultations. However, for a crude estimate we also used the mean burst rate of $\sim$2 per day, as observed during the 1999 August to October BeppoSAX Wide Field Camera campaign (Muller et al. 2000, in preparation). All burst parameters are also shown in Table 1.

Table 1. Persistent emission and burst properties

Persistent emission[a]			
	before burst	after burst	unit
$N_{\rm H}$[b]	1.7	1.7	10^{22} atoms cm^{-2}
$F_{\rm pers}$[c]	1.2 ± 0.2	1.2 ± 0.2	10^{-8} erg s^{-1} cm^{-2}
$T_{\rm bb}$	1.34 ± 0.05	1.38 ± 0.05	keV
$R_{\rm bb}$[d]	4.5 ± 0.3	4.3 ± 0.3	km
Γ	1.2 ± 0.3	1.2 ± 0.3	
$E_{\rm cut}$	4.9 ± 0.9	4.7 ± 1.0	keV
Norm.[e]	1.5 ± 0.3	1.5 ± 0.3	
$\chi^2_{\rm red}$/dof	1.62/35	0.83/35	
Burst parameters			
$F_{\rm peak}$	8.1 ± 0.3		10^{-8} erg s^{-1} cm^{-2}
$E_{\rm b}$	3.52 ± 0.04		10^{-7} erg cm^{-2}
α	> 6, $\sim$1360[f]		
τ	4.4 ± 0.2		s
γ	0.17 ± 0.03		

[a] Absorbed black-body plus cut-off power-law model.
[b] Parameter fixed, see text.
[c] Unabsorbed persistent flux estimated between 0.01–100 keV.
[d] Effective black-body radius at 5 kpc.
[e] Cut-off power-law normalization (photons keV^{-1} cm^{-2} s^{-1} at 1 keV).
[f] Assuming a burst rate of $\sim$2 per day (Muller et al. 2000, in prep).

4. Discussion

The light curve and X-ray spectral behaviour of the X-ray burst in GX 3+1 observed with RXTE show clear evidence for radius expansion of the neutron star photosphere due to near-Eddington luminosities during a themonuclear runaway on the neutron star surface (for a review see e.g. Lewin et al. 1993). The total time for the expansion and contraction phase is only $\sim$1.5 s, during which the radius expanded only by a factor of $\sim$2. Such short bursts with small expansion phases have been seen in other bright X-ray sources, such as Cyg X-2 (Smale 1998). The gradual softening at the end of the burst is attributed to cooling of the neutron star surface, which is characteristic for type-I bursts (Hoffman et al. 1978).

During the burst our derived black-body temperatures are smaller, whereas our inferred black-body radii (all at the same assumed distance) are larger, than reported for previous GX 3+1 bursts (Makishima et al. 1983, see also Inoue et al. 1981; Asai et al. 1993; Molkov et al. 1999). The burst parameter values for γ ($\sim$0.10–0.20) and τ (4–8 s) quoted by Asai et al. (1993), and inferred from the observations presented by Makishima et al. (1983) and Molkov et al. (1999), are similar to our findings. We note (see also Asai et al. 1993) that γ, τ and our estimate of α fall on the extreme end of relations between τ vs. γ and α vs. γ as presented by Van Paradijs et al. (1988) for typical type I bursters. This shows that if bright sources burst, the burst duration tends to be short (order of 10 s; note however, that some bursts in the bright "Z" source GX 17+2 have a duration of the order of minutes, see e.g. Kuulkers et al. 1997 and references therein). It is interesting to note that our X-ray burst from GX 3+1 is very similar to the radius expansion burst seen in Cyg X-2 with RXTE in most of its facets, except notably for the γ being a factor 4.3 larger for Cyg X-2 (Smale 1998). Note also that during the burst from Cyg X-2 no evidence for pulsations was reported, similar to what we conclude for GX 3+1, both with upper limits on the modulation strength which are significantly lower than for bursts during which oscillations were seen (see Strohmayer 1998, 2000).

A convenient way to display the burst properties as they vary in time, is a flux-temperature diagram, see Fig. 4. In such a diagram the phases of expansion/contraction and subsequent cooling of the neutron star photosphere are distinguished by two separate tracks (see e.g. Lewin et al. 1993). GX 3+1 moves from the middle bottom to top left (rising phase), top middle (expansion phase), back towards top left (contraction phase), and finally to the lower right part of the diagram (cooling phase). We can adequately fit ($\chi^2_{\rm red}$/dof = 0.9/34) $\log F_{\rm bol}$ versus $\log T_{\rm bb}$ during the cooling phase of the burst by a straight line with a slope of 3.97$\pm$0.15 (dotted line in Fig. 4). This means that $F_{\rm bol}$ is consistent with being proportional to $T^4_{\rm bb}$, which indicates that the neutron star photosphere radiates as a black-body during the cooling phase, at a constant radius $R_{\rm bb}$. We note that burst spectra are generally not described by pure black-body radiation, especially near the Eddington limit (see Lewin et al. 1993, and references therein). Instead the black-body ra-

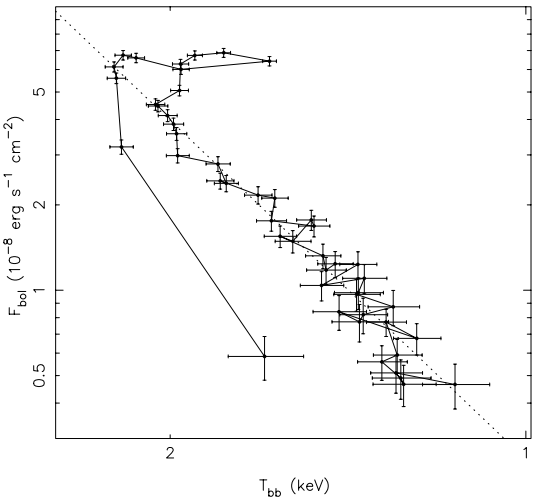

Fig. 4. Bolometric black-body flux ($F_{\rm bol}$) versus black-body temperature ($T_{\rm bb}$) for the first 14 s of the burst. Data points are connected for clarity. The dotted line represents the fit to the cooling track of the burst, see text. Note that $T_{\rm bb}$ runs from right to left.

diation is modified mainly at energies below ∼3 keV and above ∼10 keV. Since our burst spectra are analysed in the 2.9–20 keV energy range, we are, therefore, not greatly affected by modified black-body radiation. Note that we then probably underestimate our bolometric fluxes.

At the start of the expansion phase the black-body bolometric flux and temperature values do not match those at the end of the contraction phase. Our estimated emission areas are the same at these instants; the above then means that the photosphere is cooler at the end of the contraction phase with respect to the start of the expansion phase. From Fig. 4 we see that $F_{\rm bol}$ drops below the constant peak flux before the end of the contraction phase. We infer that the cooling phase therefore already started before the end of the contraction phase.

Using the fact that during the expansion and contraction phase of the neutron star photosphere the burst luminosity equals the Eddington luminosity one can get an estimate of the distance (see e.g. Lewin et al. 1993). Assuming standard burst paramaters (isotropy, cosmic abundances and a canonical neutron star mass of $1.4\,{\rm M}_{\odot}$) and taking into account gravitational redshift effects we find $d = 4.5 \pm 0.1$ kpc. If we assume a neutron star mass of $2.0\,{\rm M}_{\odot}$ we instead find $d = 5.1 \pm 0.1$ kpc. For bright sources like GX 3+1 most of the hydrogen content is being burned persistently, so during the expansion/contraction phase the neutron star atmosphere is likely to lack hydrogen. Using the Eddington luminosity appropriate for hydrogen-poor matter then leads to $d = 6.1 \pm 0.1$ kpc. Dropping only our assumption that the burst radiates isotropically, and assuming anisotropy values of $0.5 < \xi < 2$ (e.g. van Paradijs & Lewin 1987), we derive distances between 3–7 kpc. On the other hand, if the peak luminosities during radius expansion bursts are standard candles we can use the mean peak luminosity for such bursts seen in globular cluster sources for which the distances are known, i.e. $3.0 \times 10^{38}\,{\rm erg\,s^{-1}}$ (Lewin et al. 1993). In this case we derive $d \sim 5.6$ kpc. These distance estimates show that in principle one can get an idea of the distance to the source, but the exact value still remains rather uncertain by ∼30%.

The persistent flux during our observations is the same within a factor of ∼2 with respect to the previous reports when GX 3+1 was bursting, i.e. low (∼0.2 Crab). Using the fact that during the peak of the burst the observed (net-burst) luminosity is at near Eddington values we can now for the first time estimate the persistent flux in terms of the Eddington luminosity for the bright atoll sources like GX 3+1 (i.e. GX 13+1, GX 9+1 and GX 9+9). For GX 3+1 we find $L_{\rm pers} \simeq 0.17\,L_{\rm edd}$ (assuming the burst and persistent emission is radiated in the same directions). This is consistent with that inferred from models of X-ray spectra, i.e. $\sim 0.1\,L_{\rm Edd}$ (Psaltis & Lamb 1998).

GX 13+1 has been seen to burst sporadically (Matsuba et al. 1995), whereas no bursts have been reported for GX 9+1 and GX 9+9. This may mean that GX 3+1 and GX 13+1 are accreting near to the critical mass accretion rate at which bursts cease to occur, whereas GX 9+9 and GX 9+1 accrete above this limit. However, this does not explain the fact that some sources that are accreting at even higher rates (near Eddington), i.e. Cyg X-2 and GX 17+2, also irreglularly show bursts.

Acknowledgements. We thank Lars Bildsten, Mariano Méndez and Dimitrios Psaltis for discussions. We acknowledge the use of daily averaged quick-look results provided by the ASM/RXTE team. This work was supported in part by the Netherlands Organization for Scientific Research (NWO) grant 614-51-002.

References

Asai, K., Dotani, T., Nagase, F., Mitsuda, K., Kitamoto, S., Makishima, K., Takeshima, T., Kawabata, K., 1993, PASJ, 45, 801
Bradt, H.V., Rothschild, R.E., Swank, J.H., 1993, A&AS, 97, 355
Christian, D., Swank, J.H., 1997, ApJS, 197, 177
Hasinger, G., van der Klis, M., 1989, A&A, 225, 79
Hoffman, J.A., Marshall, H.L., Lewin, W.H.G., 1978, Nat, 271, 630
Inoue, H., Koyama, K., Makishima, K., et al., 1981, ApJ, 250, L71
Kuulkers, E., van der Klis, M., Oosterbroek, T., van Paradijs, J., Lewin, W.H.G., 1997, MNRAS 287, 495
Lewin, W.H.G., van Paradijs, J., Taam, R.E., 1993, Space Sci. Rev., 62, 223
Makishima, K., Mitsuda, K., Inoue, H., et al., 1983, ApJ, 267, 310
Matsuba, E., Dotani, T., Mitsuda, K., Asai, K., Lewin, W.H.G., van Paradijs, J., van der Klis, M., 1995, PASJ, 47, 575
Molkov, S.V., Grebenev, S.A., Pavlinsky, M.N., Sunyaev, R.A., 1999, Proc. of the 3rd INTEGRAL Workshop "The Extreme Universe", ApLC, 38, 141
Psaltis, D., Lamb, F.K., 1998, in Neutron Stars and Pulsars, N. Shibazaki, N. Kawai, S. Shibata & T. Kifune (eds.), Tokyo, Universal Academy, p. 179
Smale, A., 1998, ApJ, 498, L141
Strohmayer, T. 1998, Nucl. Phys. B. (Proc. Suppl.) 69/1-3, 129
Strohmayer, T. 2000, in Proceedings "X-ray Astronomy '99, Stellar Endpoints, AGN and the Diffuse X-ray Background", Bologna, Italy, in press (astro-ph/9911338)
van Paradijs, J., Lewin, W.H.G., 1987, A&A, 172, L20
van Paradijs, J., Lewin, W.H.G., 1985, A&A, 157, L10
van Paradijs, J., Penninx, W., Lewin, W.H.G., 1988, MNRAS, 233, 437